POLAR AND CHEMICAL DOMAIN STRUCTURES OF LEAD SCANDIUM TANTALATE (PST)

PENG JuLin and L.A. BURSILL

School of Physics, The University of Melbourne, Parkville, 3052, Vic. Australia

Received to be inserted
Revised to be inserted

The local structure of chemical and polar domains and domain walls is determined directly by atomic resolution high-resolution electron microscopy (HRTEM). Thus the Pb Ta and Sc atomic positions may be located in the images of very thin crystals. Furthermore the Pb cation displacements away from the ideal perovskite A-site have been measured directly for the first time. Local variations in polarization direction may be mapped directly off the images, provided certain electron optical conditions are met. The results are relevant to recent theories of polar-glass behaviour in relaxor-type complex oxide functional ceramics.

1. Introduction

Polar and chemical domain textures on nanocrystalline length scales are believed responsible for the diffuse phase transitions and unusually high dielectric response exhibited by so-called relaxor-type ceramic materials[1,2,3]. Thus the permittivity may reach values greater than 30,000 over a useful range of temperature for lead scandium tantalate (PST), depending on appropriate ceramic processing routes (see e.g. Refs.1,2). The unusual dielectric properties have been linked theoretically to chemical inhomogeneities presumed to exist due to chemical disorder of e.g. Sc and Ta site occupancies in the perovskite (ABO_3) B site. This was the classical theory due to Smolenski[4], see also Ref.[5] for an overview.

Most recently there have been intensive efforts to apply spin glass theory, originally developed for magnetic glasses, to explain relaxor-like behaviour; Cross[1] and Viehland[6,7,8,9] being the principal exponents. Note, however, that whatever theoretical approach is adopted, a point is reached where it is necessary to make assertions concerning the atomic structures underlying the extremely high density of polar and chemical domains and, of equal importance, the domain walls existing in this material.

High-resolution transmission electron microscopic (HRTEM) studies[10] of the relaxor-like material known as PST; i.e., lead scandium tantalate $Pb(Sc_{0.5}, Ta_{0.5}O)_3$ showed significant new results: including the observation of a hierarchy of nanodomain textures, observed by conventional and high-resolution dark-field imaging techniques. Furthermore the first direct measurement of the magnitude of the Pb atom shifts, with respect to those of Ta and Sc, was achieved. In addition, local

variations in microdomain dimensions and polarization directions were visualized.

In this paper we present a systematic analysis of the electron optical images of chemical and polar nanodomain textures in ordered PST, using computer simulation and image-matching techniques, and including information from digitized images and the corresponding power spectra. The Pb, Ta and Sc atomic columns are first identified. The local direction and magnitude of the Pb atom shifts are then determined. Finally, it is possible to discuss some of the local atomic structures of both chemical and polar domain walls. The results are relevant to a discussion of the classical versus the polar-glass theoretical models for relaxor-type dielectric response.

2. Experimental

An ordered specimen of PST was prepared at the Departement de Ceramique, EPFL-Lausanne. It was classified as containing sufficient PbO for the perovskite phase to be fully stoichiometric (see Chu, Reaney and Setter[11]). The long-range chemical order parameter may be defined as

$$s^2 = (I_{111}/I_{200})/(I_{111}/I_{200})_{(s=1)} \qquad (1)$$

where I_{111} and I_{200} refer to powder X-ray diffraction intensiti es for the pseudocubic 111 and 200 Bragg beams.The long-range order parameter was measured to be s = 0.93. This was the most ordered specimen available to us. Thin edges of this specimen were examined at the University of Melbourne, using a JEOL-4000EX electron microscope operating at 400KeV. The ultra-high resolution pole-pieces had Cs = 0.94mm. The three principal zone axes $< 100 >$,$< 110 >$ and $< 111 >$ of PST were accessible using double-tilt ($\pm 20°$) top-entry goniometer. All of the results reported below refer to $< 110 >$ zone axes.

The specimen height was carefully adjusted to an optimum focussing current, when the objective lens astigmatism, as well as the optical alignment parameters could be set precisely against calibrated values. The adjustment of the desired crystal orientation was achieved using a Gatan TV camera and image-intensifier. A video cassette recorder was used to record dynamic events, for both HRTEM and dark-field imaging conditions. Special attention was paid to minimizing the effects of mechanical vibrations and acoustic interference, enabling point-to-point resolutions of better than 0.17nm to be achieved at the Scherzer defocus image condition. Computer-simulated images were obtained using Melbourne University Multislice (MUM) software.

3. Results

Figure 1 shows a HRTEM image of ordered PST (referred to below as pst-o) viewed in the $[1\bar{1}0]$ projection. The corresponding electron diffraction pattern is inset. This ordered specimen gives apparently a perfect structure image across the field of view. It is shown below that there are nevertheless microcrystalline regions associated with chemically ordered and also polar domains. These features will emerge as the analysis proceeds below.

4. Analysis of HRTEM Images

4.1 Introductory

Principles for analysis of the HRTEM images and the corresponding nanodomain textures were first established by careful comparison of computer- simulated images with selected areas of the experimental images. We start with the known structure for the chemically-ordered phase, based on space group Fm3m. Then we determine by image-matching the values of the relevant electron optical parameters, e.g. crystal thickness and objective lens defocus values, for the ordered structure image. According to the weak phase object approximation, for a very thin crystal, the images most resemble the crystal structure when the objective lens current is set to the Scherzer defocus. Then the regions of low (dark) intensity in the images correspond to the projection of columns of atoms in the structure. In the case of PST we then establish that the variation of intensity corresponding to columns of different types of atoms may carry a one-to-one correspondence with the different species of atom in the ordered structure. Furthermore it then becomes possible to measure directly the Pb atom shifts with respect to the Ta and Sc atoms. Finally the atomic structures of some polar domain walls are analyzed.

4.2 Computing Facility

Selected images were digitized from high-quality prints of electron micrographs or directly from negatives using a Wild-Leitz macroscope fitted with a television camera. A 256 level grey scale with 512×512 pixels was used to input images to an IBM RISC 6000 computer via a PCVISION Frame Grabber. It was found convenient to obtain the Fourier transforms (FT) and power spectra (PS), as well as output the digitized image, using SEMPER image-processing programs

(SYNTRONICS Cambridge, UK). Images were output using a QMS 600 dpi laser-printer with 64 grey levels.

4.3 Computer Simulation Techniques

The calculations were based on the physical optics approach to electron diffraction and imaging[12]. All the nonlinear N-beam dynamic scattering, as well as lens aberrations and Fresnel propagation effects of the objective lens were included. Periodic continuation methods, as developed for atomic resolution images were obtained using MUM (Melbourne University Multislice) software.

4.4 Structural background

PST has the perovskite ABO_3 structure shown in Fig.2a, where the corner-shared BO_6 octahedra enclose the larger A cation. The chemically-disordered simple cubic Pm3m structure (a= 4Å) is usually assumed to have random occupancy of the B sites by Ta and Sc atoms (shown in Fig.2b for the <110> projection). If the Ta and Sc atoms order on alternate {111} planes the unit cell is doubled (a'=8Å) when the space group becomes Fm3m (refer to Fig.2c). At liquid nitrogen temperatures the "ordered" structure was reported to be trigonal[13]. However there have not been any definitive structural studies reported for ordered or disordered PST. Note that the complex polar and chemical domain textures are not readily analyzed using Rietveld powder diffraction techniques; also single crystals have not been available.

The space group was taken as R3, with pseudocubic cell parameters a = 0.80 nm. Initially, ideal atom coordinates were transformed from the Fm3m ordered PST structure. In the course of the analysis several series of Pb atom shifts, consistent with R3 space group symmetry were deduced for the image simulation. The effects of oxygen shifts were investigated by applying shifts antiparallel to the best-fit Pb shifts and having one-third the magnitude of the latter. In fact, the image simulations showed that there were no detectable effects of the oxygen shifts on the set of images under discussion.

4.5 Structure image of ordered microdomains (s=1)

Figure 3 shows (top) the transmitted intensity of the 1/2(111) superlattice reflection for increasing crystal thichness, corresponding to the [110] zone of Fig.1. Some typical computer-simulated HRTEM images are given at the bottom part of

Fig.3. Note that a so-called "structure-image" occurs only for the thinnest crystal (1.25nm) at close to the Scherzer defocus condition (defocus of 50nm). In this case the dark spot intensity bears a one-to-one relationship to the Pb, Ta and Sc atom columns. For increasing crystal thickness the superlattice spots increase in intensity and the images develop a diamond shaped periodicity typical of ordered pst.

An enlarged HRTEM image selected from the very thin edge of Fig.1 (labeled A) is shown in Fig. 4a. Inset (a) is the power spectrum of the selected image, (b) is a computer-simulated image match and (c) is the corresponding power spectrum (equivalent to the Fraunhofer diffraction pattern) of inset (b). Under the Scherzer defocus condition, the image contains three distinct levels of black spot intensities which have one-to-one correspondences to Pb (z=82), Ta (z=73) and Sc (z=21) atoms respectively. It should be possible therefore to see directly whether Ta and Sc atoms order on alternate {111} planes. In order to investigate this further the image intensity profile along adjacent [110] atomic rows was scanned along the [001] direction of both the digitized experimental image (Fig.4) and the corresponding computer-simulated image (Fig.4b). The results are given in Fig.5a and Fig.5b for the simulated and experimental images respectively. In Fig.5a the Pb atom row showed relatively uniform intensity whereas the (Ta,Sc) atomic rows show two levels of intensity, with the darker level corresponding to Ta. For Fig.5b we note first of all that there are shifts of the Pb atom positions which were not evident for the simulated image (Fig.5a). This is because the simulation was made for an ideal perovskite unit cell. We return to discuss shifts below. Note that there is of course significant noise for the experimental images. Background intensity variations also occur. Nevertheless the experimental atom row profiles do show the expected intensity levels, in good agreement with the simulated profiles. which clearly demonstrates that Fig.4 represents a structure image of a fully ordered chemical microdomain. This is the first time such direct evidence for the chemical ordering of Ta and Sc in B sites of a perovskite structure has been obtained.

Some variations of intensity at Pb atom positions are visible in Fig.5b. These are presumedly due to some deficit of Pb, which is known to occur readily during preparation of this material[11], or perhaps during the HRTEM observations, although the latter did not appear to be noticable. Further study of Pb deficit related defects including Pb or PbO vacancies, platelet defects (loops), stacking faults, helical dislocations, and voids facetted on (111) and (110) planes, will be discussed elsewhere (Peng et al[14]).

It remains to determine the magnitudes and directions of the Pb atom shifts evident in Fig.4(b). Figs.6(a-d) show enlargements of a thin area of the ordered specimen, where the dark spots may be identified with the Pb, Ta and Sc atom positions. The lower diagram identifies the atom columns, as verified exactly by computer simulated images. Simulated images were obtained corresponding to Pb shifts of 0.0, 0.2, 0.4, and 0.6Å, along a <111> direction. The computed images

are shown in Fig.7(a-d). Note that in this case the Pb atom shifts lie parallel to the image plane, i.e. perpendicular to the projection axis [110]. Note also that 0.015nm shifts have been assumed for both Ta and Sc atoms. It was not possible to match the experimental images for Pb shifts of less than 0.05nm. Thus the Pb shift, relative to Ta and Sc atoms, is approx. 0.035nm. Note that there may be additional antiparallel shifts of the oxygen atoms, which are not imaged here. The structure model used is actually almost identical to the structure proposed for ferroelectric lead zirconium titanate (PZT); of course here the Sc and Ta cations are ordered, whereas for PZT Zr and Ti cations are disordered over the perovskite B sites. Reference should be made also to the paper of Darlington and Megaw[15], which gives a quite general systematic analysis of the possible rhombohedral structures derived from perovskite high-temperature aristotypes.

4.6 Determination of local polarization characteristics

If we assume R3 space group symmetry for polar nanodomains, as resulted from the analysis of Figs.6,7 above, then there are in principle eight such domains expected to form within the high-temperature Pm3m average structure. Fig.8 shows the corresponding atomic projections along a $[10\bar{1}]$ pseudocubic direction. Note that four cases arise with polarization vector P_s lying in the plane of the figure; the remaining four cases, where P_s projects along [001] or $[00\bar{1}]$, give only two distinct projections. The directions of P_s are indicated on Fig.8. Some consideration of this figure reveals that there are essentially two types of atomic projection which should appear in the HRTEM images. The first case was analysed in Fig.6; it showed zig-zag lines parallel to [001], corresponding to the sequence Pb-Sc-Pb-Ta-Pb-, where the Pb shifts lie in the plane of the drawing along one of [111], $[\bar{1}\bar{1}\bar{1}]$, $[\bar{1}\bar{1}1]$ or $[11\bar{1}]$. The second case should give a long-short-long-short sequence for Pb-Sc-Pb-Ta-Pb- along [001], where the Pb shifts are along $[\bar{1}11]$, $[1\bar{1}\bar{1}]$, $[1\bar{1}1]$ or $[\bar{1}1\bar{1}]$. A search of the HRTEM structure images quickly revealed the two distinct classes of image. An example of the second case is given as Fig.9; the Pb shifts are indicated. Note that Fig.9 was obtained from the same negative as Fig.6; thus two polarization vectors coexsist within a single chemically-ordered domain, implying the existence of polar domain walls.

Fig. 8 also shows schematically some of the many possible polar domain walls (PDW) which may exist for $[10\bar{1}]$ zone axis projections of pst-o. A systematic structural and diperiodic symmetry group analysis reveals that the PDW may be neutral, positively or negatively charged, depending on the relative directions of the polarization vectors connected across the different domain walls. Of course Fig.8 assumes that the PDW are exactly parallel to either (001) or (110) planes, which is likely to occur to a significant extent, but by no means exclusively. A search for

HRTEM images showing atomic structure images of PDW is continuing.

5. Conclusion

It has been shown above that Pb, Ta and Sc atomic columns may be identified directly by use of HRTEM images of PST, provided the edge of the crystal is sufficiently thin.

The local magnitude and direction of P_s may also be assigned directly by careful analysis of the HRTEM images in favorable cases; for example where we have a single chemically-ordered domain containing two or more non-overlapping polar domains. Such was the case for Figs.6,9 which refer to ordered pst.

We may conclude by asserting that the atomic structure of both chemical and polar domains have been observed directly and the polarization vectors have been characterized for ordered pst. A statistical analysis of polar domain size and polarization direction has not been achieved as yet.

Exactly similar polar nanodomains are expected to occur for the case of disordered pst; although the statisical distribution of polar domain sizes and polarization directions will be expected to differ quantitatively from that for pst-o. Of course the dynamics of polarization fluctuations will also be quite different, depending critically on the local chemical disorder.

Identification of the polarization vector (P_s) for polar domains in chemically-disordered specimens is also possible, although the probability of finding non-overlapping polar domains in these cases is very restrictive. Dynamical fluctuations for the latter further complicate the analysis, which requires painstaking scrutiny of video recordings of the HRTEM images. We are presently developing on-line image processing techniques to meet the challenge of this problem.

The value of electron-optical imaging techniques for obtaining chemical microdomain structural information has been clearly demonstrated for PST. The results offer new insights into the physics and chemistry of relaxor materials and also possibilities to explore the width and structures of chemical and polar walls at atomic level. The relationship between these results and the physical properties of this interesting material will be presented elsewhere (Qian, Peng and Bursill[16]). It is also important to realize that there are limitations on the computer simulated images at present. Thus it will be necessary to include nonzero short-range order in the structural models; this is presently being attempted using Monte Carlo and NNN-Ising model simulations of chemically disordered pst, which provides a realistic set of atomic coordinates which may be input into the image simulation programs (Qian, Peng and Bursill[17]).

Acknowledgements

This work was supported by the Australian Research Council. We are grateful for the use of the JEOL-4000EX ultrahigh resolution instrument provided at the University of Melbourne, known as the National Advanced Materials Analytical Centre or NAMAC. We also thank Peter O'Brien for his guidance in the Baker Computation Laboratory. We also acknowledge the enthusiastic support of Professor Nava Setter, Chu Fan and Dr. Ian Reaney, of the Labo. de Ceramique, Ecole Polytechnique Federal de Lausanne, Switzerland.

References

1. L.E. Cross, *Ferroelectrics*, **76**, 241-267 (1987).
2. N. Setter and L.E. Cross, *J.Mat.Sci.*, **15**, 2478-2482 (1980).
3. N. Setter and L.E. Cross, *J.Appl.Phys.*, **51**, 4356-4360 (1980).
4. G.A. Smolenskii and V.A. Isupov, *Soviet Journ. Tech. Physics.* , **24**, 1375-1379 (1954).
5. G.A. Smolenskii, *J.Phys.Soc.Jap.(suppl.)*,, bf 28, 26-37 (1970).
6. D. Viehland, S.J. Jang, L.E. Cross and M. Wuttig, *J. Appl. Phys.*, **68**, 2916-2921 (1990).
7. D. Viehland, Wuttig, M. and L.E. Cross, *Ferroelectrics*, bf 120, 71-77 (1991).
8. D. Viehland, S.J. Jang and L.E. Cross, *Philos. Mag.*, [B64, 335-344 (1991).
9. D. Viehland, S.J. Jang, L.E. Cross and M. Wuttig, *J.Appl.Phys.* , **69**, 414-419 (1991).
10. L.A. Bursill, J.L. Peng, F. Chu, N. Setter and Ian Reaney, *Ferroelectrics*, in press (1992).
11. F. Chu, Ian Reaney and N. Setter, *in prep.*,(1992).
12. P. Goodman and A.F. Moodie, *Acta Crystallogr.***30**, 280-291 (1974).
13. P. Groves, *J. Phys. C: Solid State Phys.***18**, L1073 (1985).
14. J.L. Peng, L.A. Bursill, F. Chu, Ian Reaney and N. Setter, *in prep.*(1993).
15. H.D. Megaw and C.N. Darlington, *Acta Crystallogr.***A31**, 161-173 (1975).
16. H. Qian, J.L. Peng and L.A. Bursill, *in preparation*(1993).
17. H. Qian, J.L. Peng and L.A. Bursill, *Inter. J. Mod. Phys.***XX** submitted (1993).

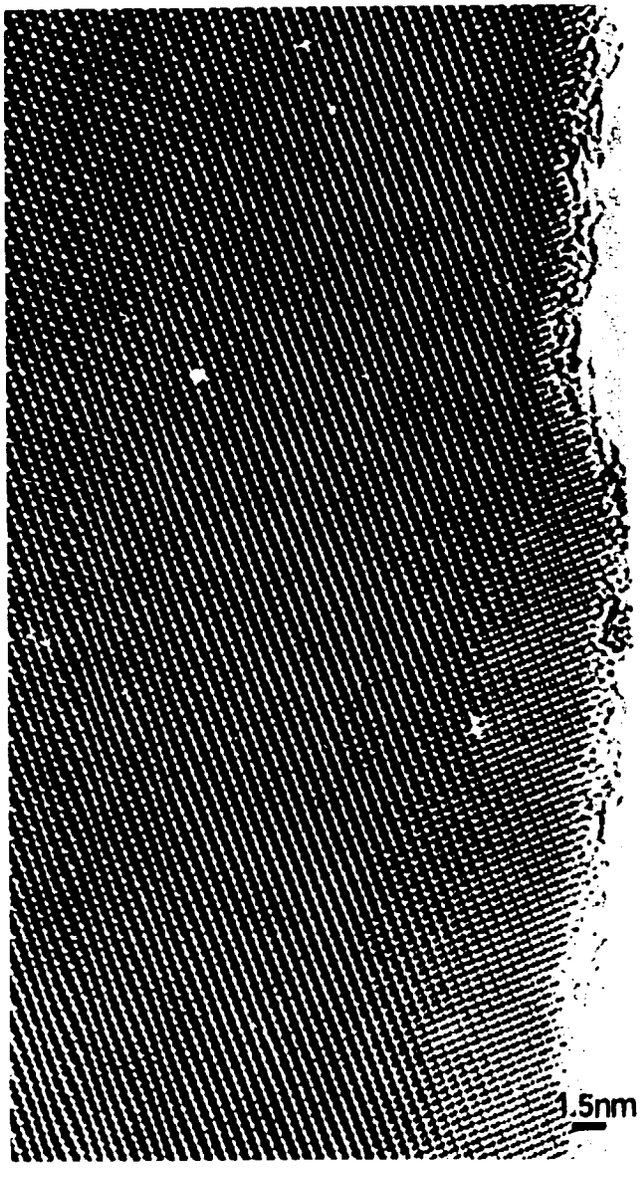

Fig.1 HRTEM image of ordered PST

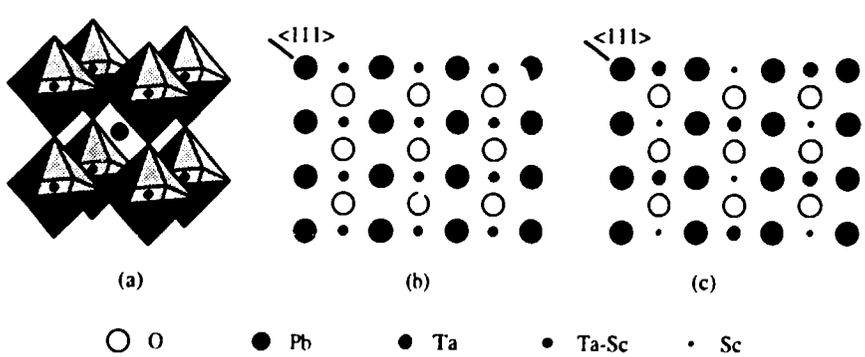

Fig.2 (a) Perspective view of the structure of PST; (b) <110> projection of disordered PST and (c) <110> projection of ordered PST.

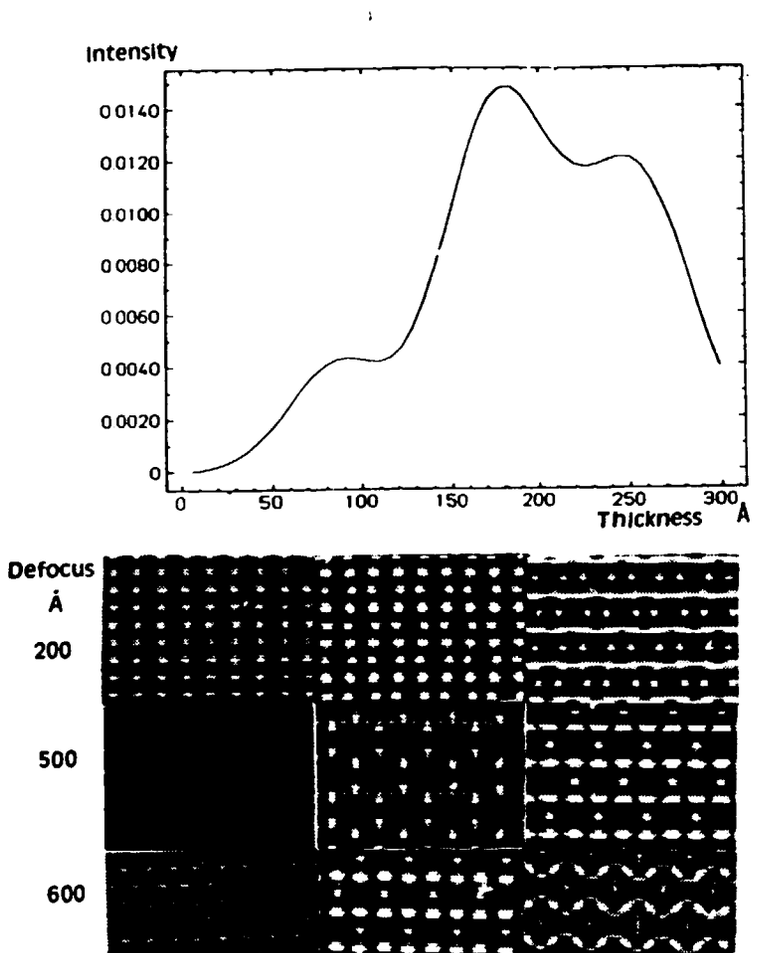

Fig.3 Intensity of 1/2(111) superlattice reflection of pst-o for increasing crystal thickness (top); typical HRTEM image simulations (lower) show structure image occurs for thickness 1.25nm and defocus of 50nm.

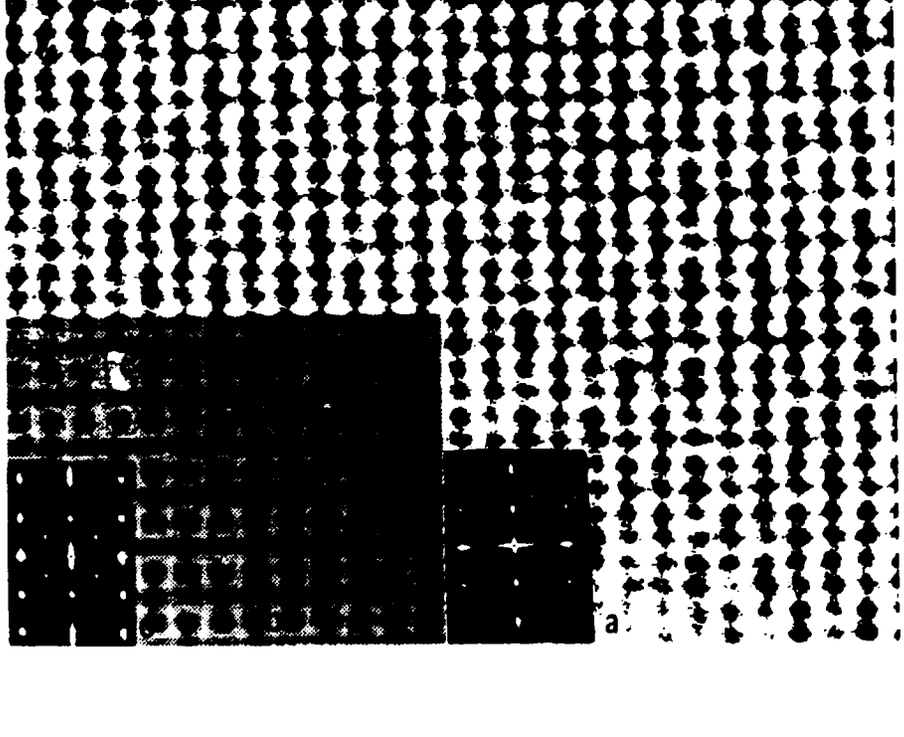

Fig.4 Structure image of ordered PST. Inset are (a) the PS of the experimental image, (b) a computer-simulated image and (c) PS of (b).

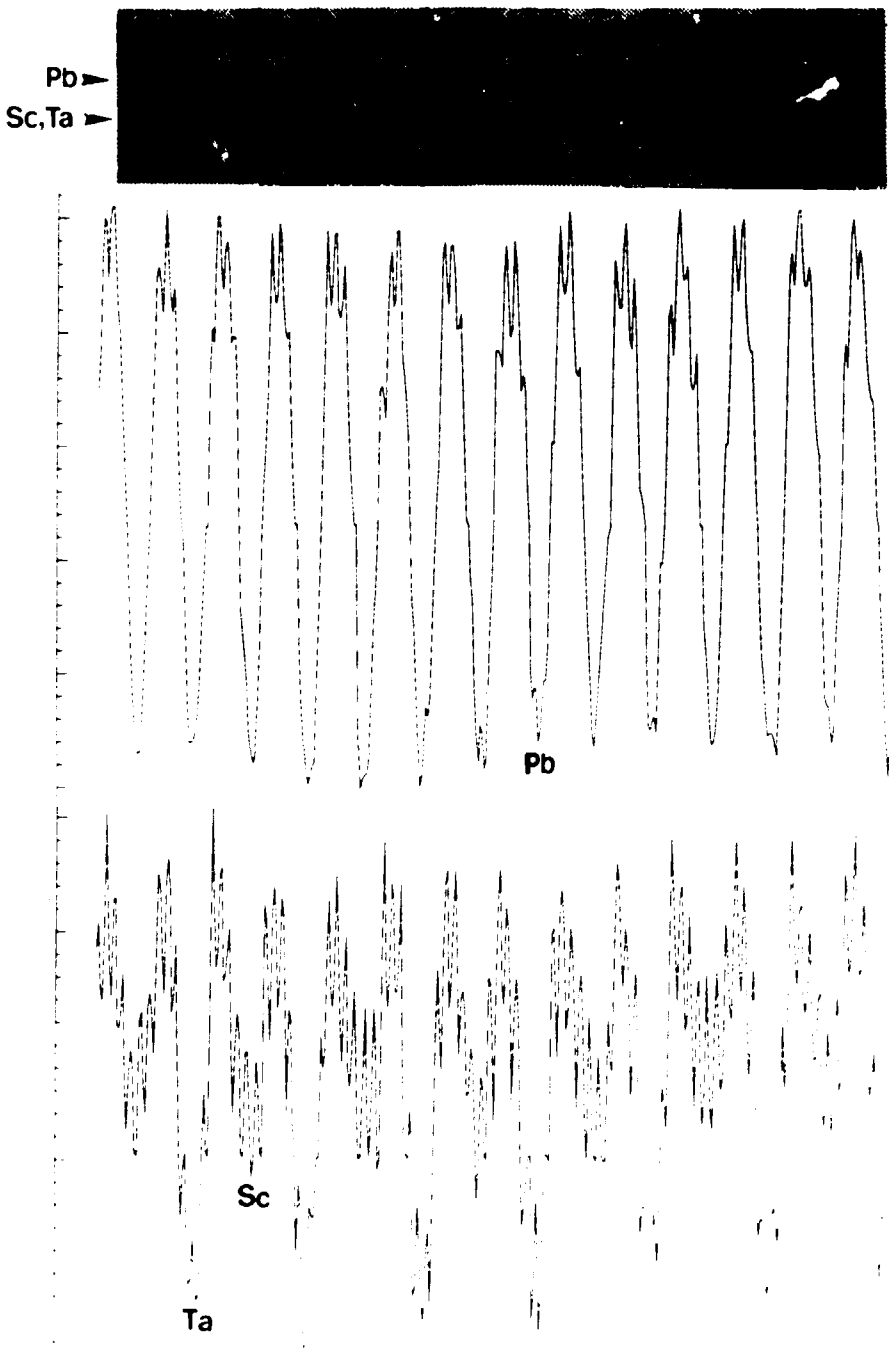

Fig.5 (a) Simulated image of pst-o (top). Pb atom rows show uniform dark intensity whereas Ta and Sc atom rows show two levels of darker intensity.

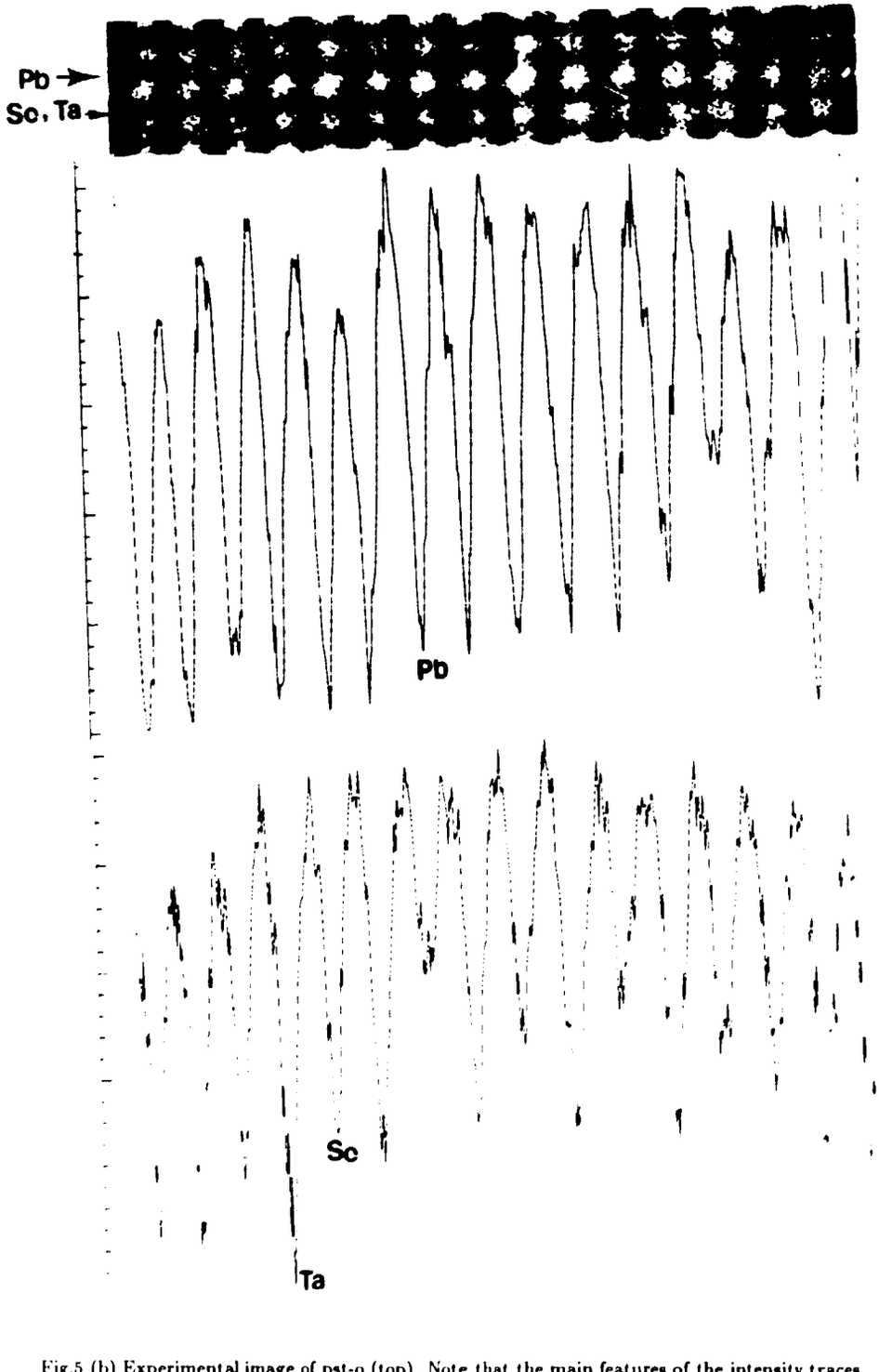

Fig.5 (b) Experimental image of pst-o (top). Note that the main features of the intensity traces agree with Fig.5(a).

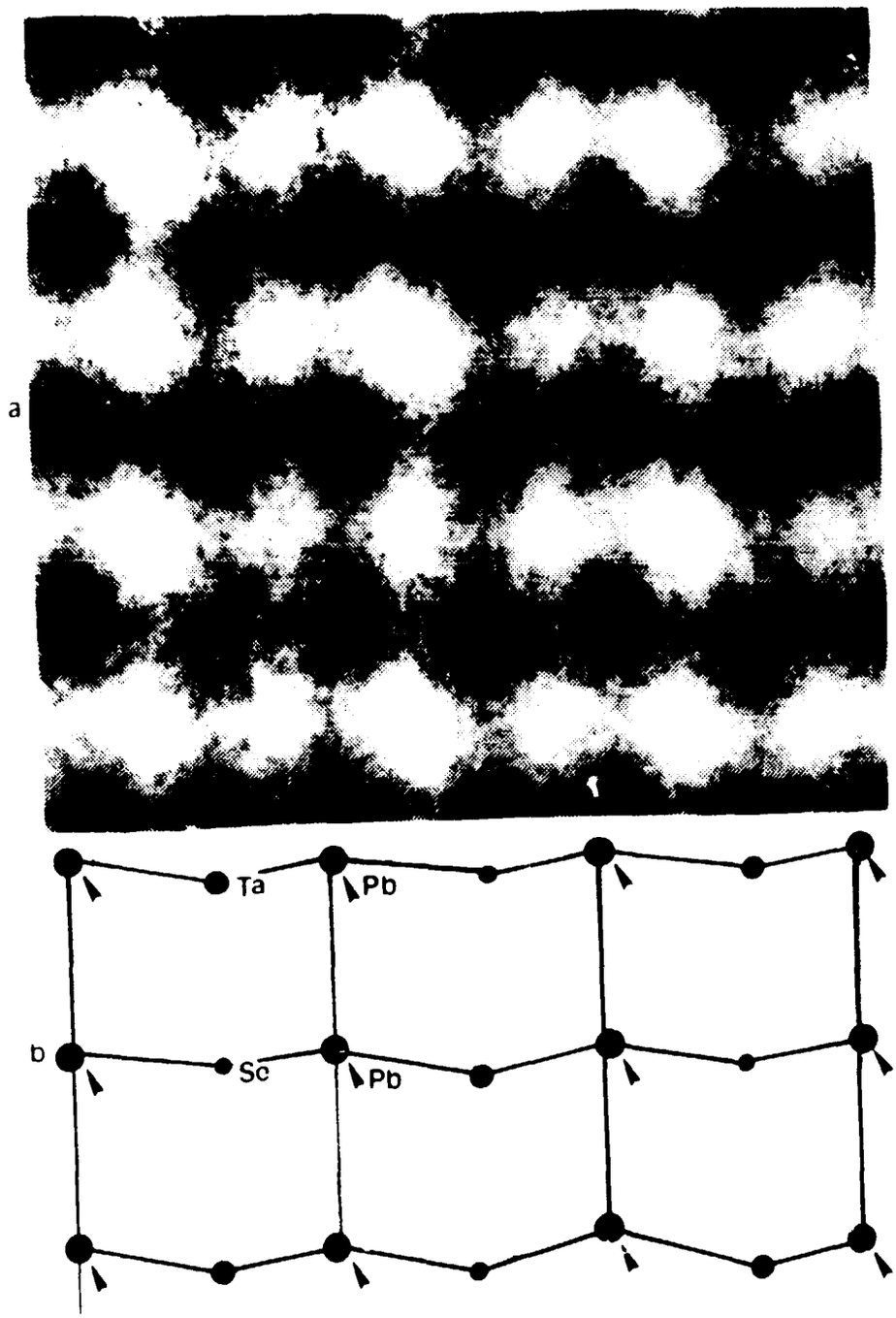

Fig.6 (a) An enlarged micrograph of ordered pst showing the effect of Pb cation shifts. (b) shows the Pb, Ta and Sc atom columns as identified by comparison with computer-simulated images.

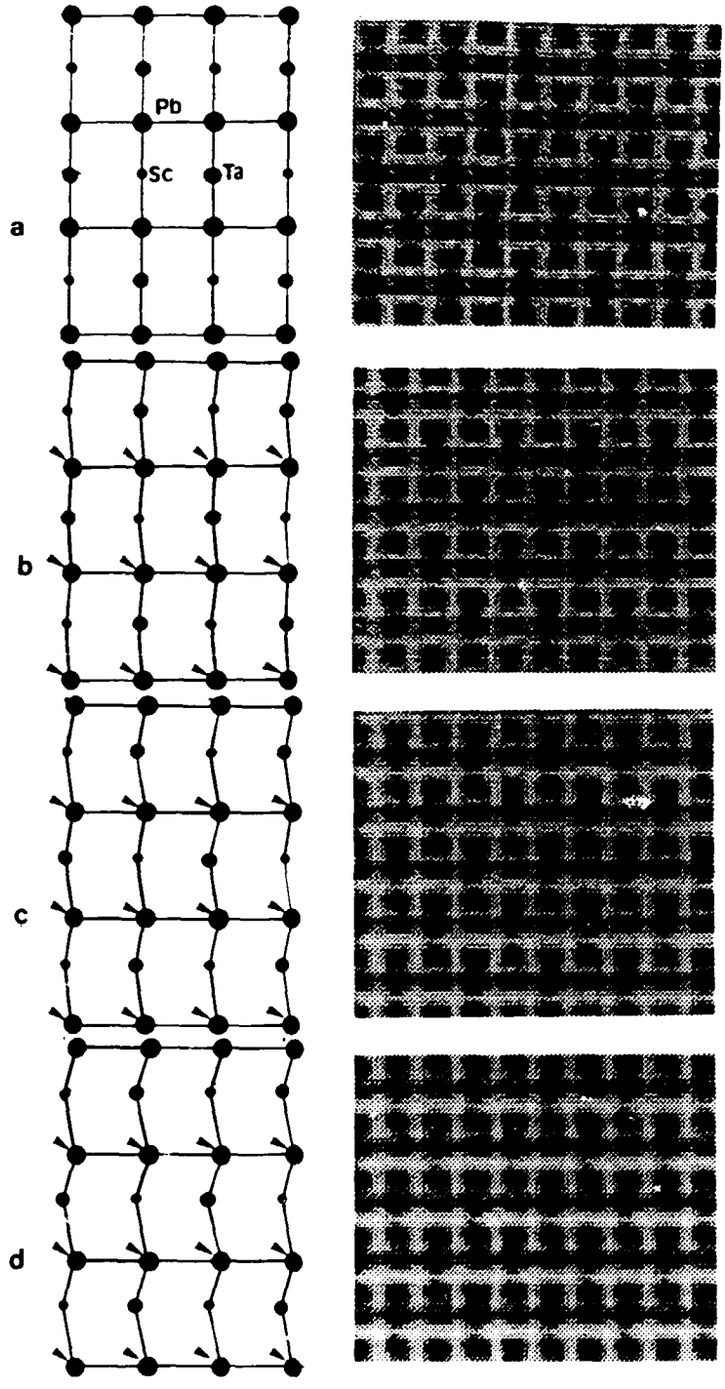

Fig.7(a-d) Computer simulated images and structural drawings showing the effects of shifting Pb atoms by 0, 0.2, 0.4 and 0.6Å respectively.

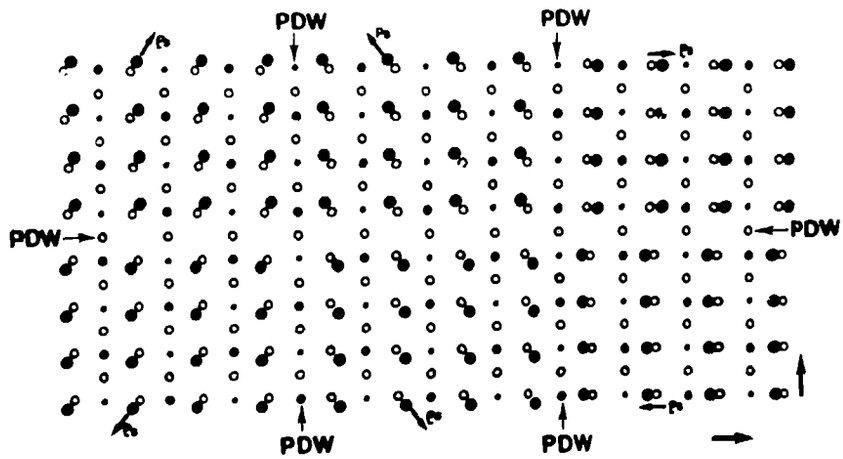

Fig.8 [101] projection of pst-o showing distinct polar domain structures. Note relative directions of Pb cation shifts and the different types of polar domain wall (PDW) structures.

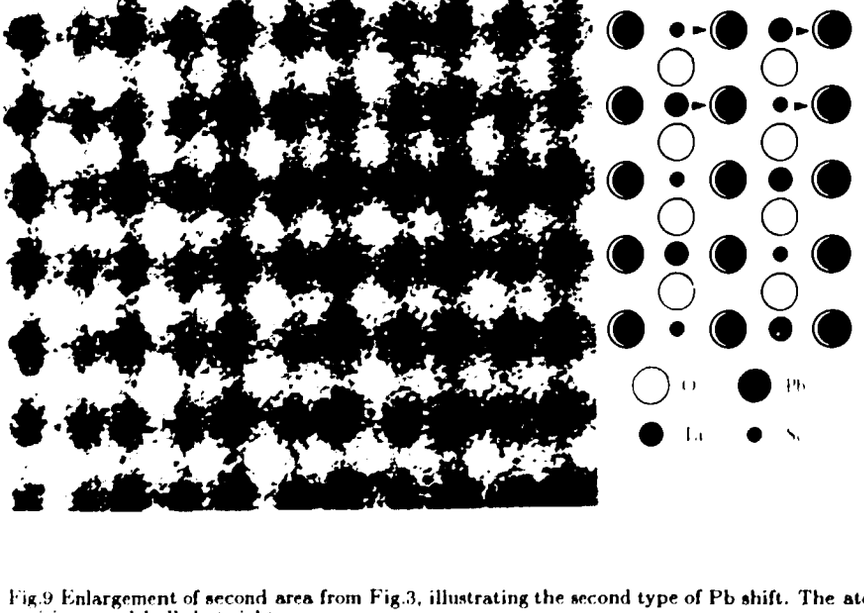

Fig.9 Enlargement of second area from Fig.3, illustrating the second type of Pb shift. The atom positions are labelled at right.